



Cite this: *Org. Biomol. Chem.*, 2017, **15**, 2459

Ratiometric electrochemical detection of hydrogen peroxide and glucose†

Sean Goggins,* Ellen A. Apsey, Mary F. Mahon and Christopher G. Frost

Hydrogen peroxide (H₂O₂) detection is of high importance as it is a versatile (bio)marker whose detection can indicate the presence of explosives, enzyme activity and cell signalling pathways. Herein, we demonstrate the rapid and accurate ratiometric electrochemical detection of H₂O₂ using disposable screen-printed electrodes through a reaction-based indicator assay. Ferrocene derivatives equipped with self-immolative linkers and boronic acid ester moieties were synthesised and tested, and, through a thorough assay optimisation, the optimum probe showed good stability, sensitivity and selectivity towards H₂O₂. The optimised conditions were then applied to the indirect detection of glucose *via* an enzymatic assay, capable of distinguishing 10 μM from the background within minutes.

Received 26th January 2017,
Accepted 21st February 2017

DOI: 10.1039/c7ob00211d

rsc.li/obc

Introduction

Hydrogen peroxide (H₂O₂) is an important small molecule used in many industrial applications, such as paper-bleaching and in the manufacture of disinfectants and explosives.¹ In nature, it has been recently established that H₂O₂ is involved within a number of crucial roles related to cell signalling.² Abnormally high concentrations of H₂O₂ can be cytotoxic to cells³ but more significantly, however, it is a precursor to the indiscriminately reactive hydroxyl radical (•OH).⁴ This, along with other reactive oxygen species (ROS),⁵ have been shown to contribute to oxidative stress, a major factor in the onset of various diseases.⁶ Additionally, H₂O₂ is produced as a by-product in numerous enzyme-catalysed processes such as the aerobic oxidation of alcohols,⁷ urates,⁸ amino acids,⁹ and certain carbohydrates,¹⁰ including glucose.¹¹ Moreover, H₂O₂ has become a popular signal propagator within signal amplification methodologies used to enhance the sensitivity of diagnostic assays.^{12,13} Since H₂O₂ can be used as a reactive biomarker for effective disease diagnosis, and disease monitoring, as well as to infer the presence of trace amounts of explosives,¹⁴ there is therefore a significant interest in the development of accurate and reliable hydrogen peroxide detection methods.

Conventional H₂O₂ detection is typically achieved through optical techniques, namely using luminescent,¹⁵ or fluorescent methods.¹⁶ However, the need for transparent samples as well as the use of expensive optical equipment, prohibits their use at the point-of-need setting. Electrochemistry is therefore gaining increasing popularity due to its low-cost, inherent miniaturisation capability and simple incorporation into point-of-care (POC) devices.¹⁷ Despite this, the adoption of electrochemical (bio)sensors into POC devices is hampered by inaccurate and unreliable results caused by a number of issues; primarily significant variations in screen-printed electrode surface areas. One method to improve the accuracy and reliability of electrochemical (bio)sensors is through the employment of dual-reporter or ratiometric detection systems. Over recent years, the electrochemical sensing community have developed a variety of such innovative protocols for the detection of DNA,¹⁸ enzyme activity,¹⁹ proteins,²⁰ heavy metals,²¹ and small molecules,²² among others.²³ Continuing our endeavour into developing ratiometric electrochemical methods towards more accurate and more reliable electrochemical biosensors, we describe herein, the development of a ferrocene-derived probe specifically designed for the facile ratiometric electrochemical detection of H₂O₂ and demonstrate its application towards a reliable electrochemical glucose chemodosimeter.

Department of Chemistry, University of Bath, Claverton Down, Bath, BA2 7AY, UK.

E-mail: s.goggins@bath.ac.uk

† Electronic supplementary information (ESI) available: General information, materials, electrochemical methods, synthetic routes and procedures for ferrocene probes, additional differential pulse voltammograms, additional assay figures, full details of the oxidant screen and copies of NMR spectra for novel compounds. CCDC 1528331. For ESI and crystallographic data in CIF or other electronic format see DOI: 10.1039/c7ob00211d

Results and discussion

Optimisation of probe structure

H₂O₂ is itself electrochemically active but only at a high oxidation potential.²⁴ In order to decrease this overpotential and increase specificity, previous electrochemical methods for the



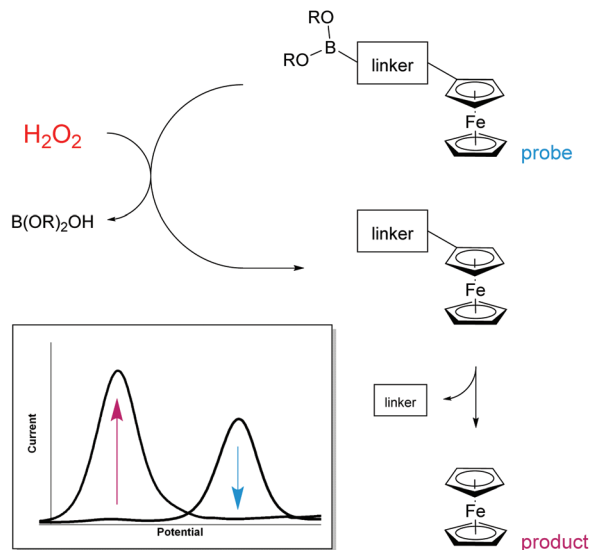


Fig. 1 Design approach towards the ratiometric electrochemical detection of hydrogen peroxide.

detection of H_2O_2 have focussed upon modifying electrodes using advanced materials.²⁵ However, the use of modified electrodes is infeasible at the point-of-need setting as they can be expensive and difficult to manufacture, and are currently unable to be easily mass produced. To obtain a ratiometric detection method at facile oxidation potentials,[‡] without the need for modified electrodes, we looked to begin our investigation by utilising ferrocene as a redox-active label. Also, by coupling a boronic acid trigger moiety into the design of the ferrocene-based probe, we hypothesised that oxidation and subsequent hydrolysis of the boronic acid trigger would only occur selectively in the presence of H_2O_2 ,²⁶ allowing for an irreversible reaction-based detection method to be achieved (Fig. 1).²⁷

Towards this end, compounds 1–5 were designed and synthesised (see ESI[†]) with the aim of identifying the optimum structural criteria needed to attain a selective ratiometric electrochemical detection method for H_2O_2 (Fig. 2). Since different self-immolative linkers exhibit different elimination kinetics in response to H_2O_2 ,²⁸ compounds 1–3 were designed to determine the linker that delivered the quickest release of an electron-rich ferrocene reporter unit. Specifically, compound 1 utilised the commonly employed *p*-benzyl carbamate linker (the definitive structure of which was confirmed by X-ray crystallography (Fig. 3)),²⁹ compound 2 contained a recently-described allyl carbamate linker,³⁰ and compound 3 contained no linker at all. Compounds 4–5, structural analogs of compounds 1–2 without the boronic acid trigger, were designed to determine and confirm that the specificity of the

[‡] Facile oxidation potentials are considered to be 0 mV (± 500 mV) vs. Ag/AgCl as this minimises the risk of interfering redox reactions from taking place and where the background current is lowest.

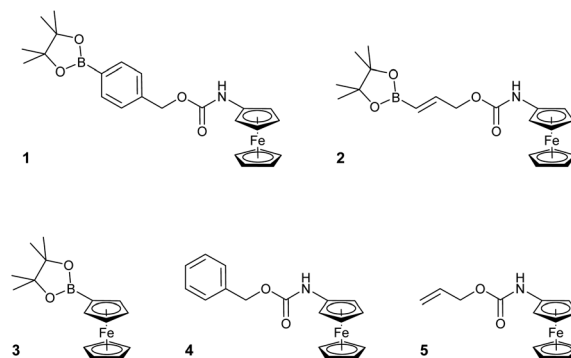


Fig. 2 Structures of ferrocene-derived ratiometric electrochemical H_2O_2 probes 1–5.

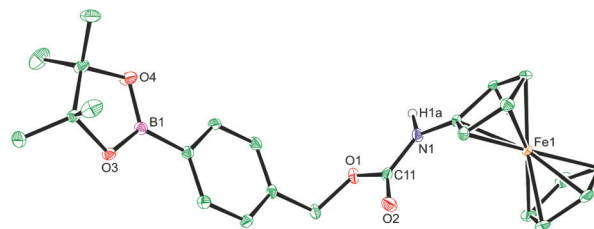


Fig. 3 X-ray crystal structure of probe 1. Ellipsoids are depicted at 30% probability and C–H hydrogen atoms have been omitted for clarity. Atom colours: C, green; O, red; B, magenta; N, blue; Fe, orange. §

reactivity towards H_2O_2 arises from the boronic acid ester trigger unit.

With probes 1–5 in hand, 100 μM concentrations of the probes in pH 8.1 tris(hydroxymethyl)methylamine (Tris) buffer were exposed to a solution containing 1 mM (10 equivalents) of H_2O_2 and the assay analysed after 20 minutes using differential pulse voltammetry (DPV). When the reaction assays regarding probes 1 and 2 were analysed, complete disappearance of the oxidation peak corresponding to the substrate and a new peak, at a significantly lower oxidation potential, was observed (Fig. 4). This peak was found to be at an identical oxidation potential as that of aminoferrocene 6, which was synthesised separately according to a literature procedure.³¹ As such, this observation of a ratiometric electrochemical detection method can be attributed to the as-designed H_2O_2 -mediated oxidation of the boronic acid moiety to its corresponding alcohol, which is followed by subsequent linker elimination and carbamate decarboxylation to release aminoferrocene 6.

§ Crystal data for compound 1. $\text{C}_{24}\text{H}_{28}\text{NO}_4\text{FeB}$, $M = 461.13$, triclinic, space group $P\bar{1}$ (no. 2), $a = 9.8839(4)$, $b = 9.9233(4)$, $c = 13.1134(5)$ Å, $\alpha = 109.219(4)$, $\beta = 93.721(3)$, $\gamma = 115.017(4)^\circ$, $U = 1068.78(7)$ Å³, $Z = 2$, $T = 150$ K, $\mu(\text{Cu K}\alpha) = 5.914$ mm⁻¹, $D_c = 1.433$ g cm⁻³, 10 333 reflections measured ($10.32^\circ \leq 2\theta \leq 143.94^\circ$), 4176 unique ($R_{\text{int}} = 0.0448$) which were used in all calculations. The final R_1 was 0.0421 ($I > 2\sigma(I)$) and wR_2 was 0.1112 (all data). CCDC 1528331 contains the supplementary crystallographic data for 1.



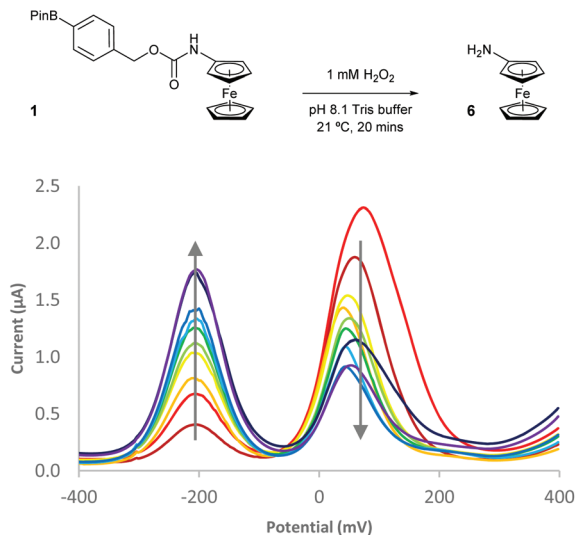


Fig. 4 Differential pulse voltammogram (DPV) overlays of probe 1 after exposure to 10 eq. of H_2O_2 .

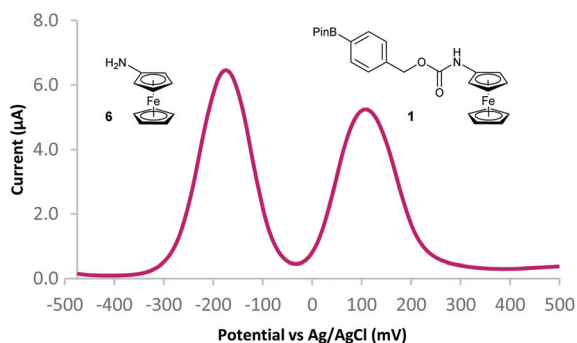


Fig. 5 DPV of probe 1 (50 μM) and aminoferrocene 6 (50 μM) in 50 mM pH 8.1 Tris buffer.

The analysis of the peroxide assay with probe 3 also revealed the disappearance of the probe peak but no expected peak at a lower oxidation potential was seen. This could be due to H_2O_2 -mediated oxidation of the ferroceneboronic acid probe 3 to hydroxyferrocene 7 but due to the known instability of 7 in aqueous conditions,³² rapid decomposition of the product occurred. When probes 4 and 5 were exposed to H_2O_2 , no peak corresponding to aminoferrocene 6 was observed showing that the carbamate functionality is stable towards alkaline peroxide and confirms that the boronic acid ester trigger moieties are essential for achieving peroxide selectivity within reaction-based assays.

Two separate equimolar solutions (100 μM total ferrocene concentration) containing probe 1 and aminoferrocene 6 (Fig. 5), and probe 2 and 6 (see ESI[†]) were analysed by DPV. Differences in oxidation potentials (ΔE_{ox}) between probe and reporter were found to be 268 mV (± 14 mV)[¶] and 232 mV

[¶] Differences in oxidation potentials (ΔE_{ox}) were calculated as the mean average from a set of 8 separate electrochemical experiments (DPV) performed on the same sample solution. \pm errors are the standard deviation from this mean ($n = 8$).

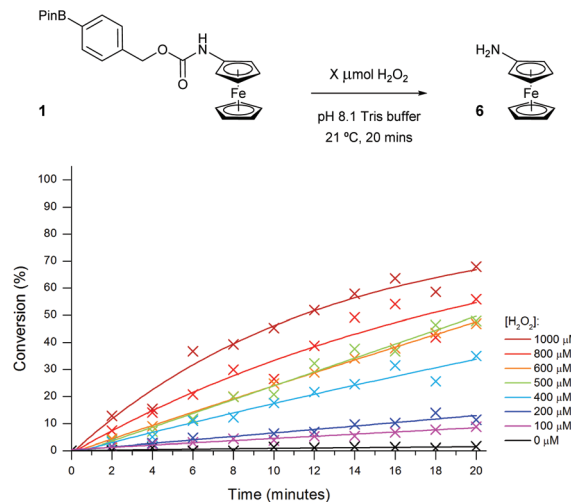


Fig. 6 Conversion of probe 1 (100 μM) to aminoferrocene 6 in 50 mM pH 8.1 Tris buffer in the presence of various concentrations of H_2O_2 .

(± 4 mV)[¶] respectively. These values can be considered more than sufficient to deliver a ratiometric detection method as an ideal difference in oxidation potential between substrate and product has previously been suggested to be between 100–200 mV to ensure both compounds are not oxidised at the same oxidation potential.³³ This allows for, through integration of the peaks on the voltammogram, reaction conversions to be calculated *via*:

$$\text{Conv. (\%)} = \frac{\int \mathbf{6}}{(\int \mathbf{6} + \int \mathbf{1})} \times 100.$$

In order to determine which probe showed the greatest reactivity towards H_2O_2 , as well as the quickest elimination kinetics, 100 μM concentrations of the probes were exposed to differing concentrations of H_2O_2 and monitored over time through ratiometric electrochemical analysis (Fig. 6 and ESI[†]). Pleasingly, all concentrations of 1 eq. H_2O_2 and higher afforded positive production of compound 6. Importantly, a <2% background rate was also observed exemplifying the excellent stability of probes with carbamate linkages in aqueous buffers. This allowed a 100 μM concentration of H_2O_2 to be determined from the background. Despite improved solubility in the aqueous medium, probe 1 was taken forward over probe 2 for further optimisation due to its increased reactivity and the greater ΔE_{ox} observed between substrate and product, which is likely caused by its increased hydrophobicity.³⁴

Assay optimisation

In order to improve the sensitivity of the assay, a number of reaction parameters were investigated. First, a range of different alkaline buffers were tested to determine if the buffer type had any effect on the reactivity of the probe. Unfortunately, any diversion away from the originally chosen Tris buffer either led to the appearance of significant artefacts



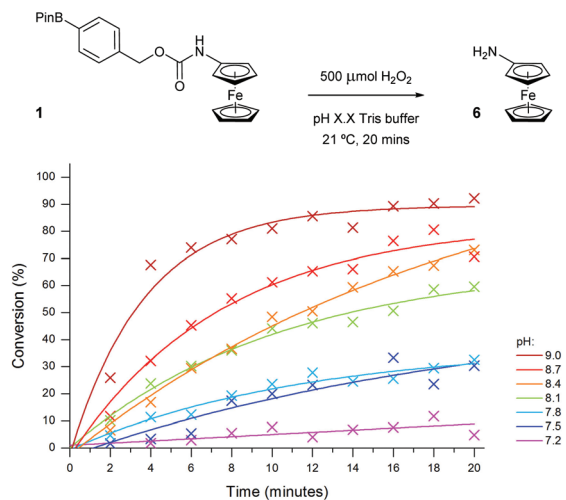


Fig. 7 Conversion of probe 1 (100 μM) to aminoferrocene 6, varying the pH of 50 mM Tris buffer in the presence of 500 μM of H_2O_2 .

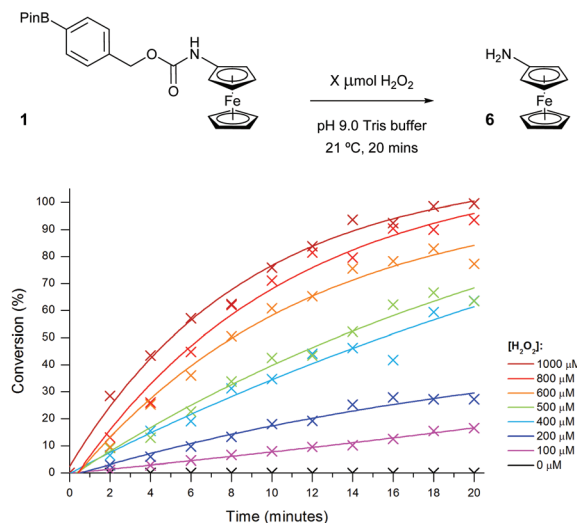


Fig. 8 Conversion of probe 1 (100 μM) to aminoferrocene 6 in 50 mM pH 9 Tris buffer in the presence of various concentrations of H_2O_2 .

on the voltammogram or caused substantial decomposition of the ferrocene probes. As such, ideal like-for-like comparisons could not be made since accurate peak integrations, and therefore precise reaction conversions, were unable to be obtained.

The pH of the assay was next to be studied since peroxide reactivity and linker elimination can both be affected through changes in pH.³⁵ The useful working pH range of Tris buffer is 7–9 and as such, the assay was conducted at various pH values within this range (Fig. 7).³⁶ As expected, decreasing the pH of the assay medium led to a significant reduction in conversion due to the shift in equilibrium from the hydroxide anion (HOO^-) to its neutral species (H_2O_2) and also due to the increase in stability of the resultant phenol intermediate post-oxidation of probe 1. Increasing the pH above 8.1 had the desired effect of enhancing the reactivity of H_2O_2 towards probe 1, enabling near quantitative conversion to aminoferrocene 6 to be obtained within 20 minutes in the presence of 500 μM (5 eq.) of H_2O_2 .

Finally, in a bid to improve the sensitivity of the assay further, the temperature of the reaction was next to be looked at (see ESI†). Increasing the temperature of the assay from room temperature to 37 $^\circ\text{C}$ was found to only slightly increase reaction conversion. Increasing the temperature further led to a dramatic rate increase with near quantitative conversions being obtained within 20 minutes in the presence of only 250 μM (2.5 eq.) H_2O_2 . However, at these elevated temperatures, fluctuating conversions can be seen thought to be due to the slow disappearance of the aminoferrocene 6 product peak and thus indicating decomposition of the product. This can be rationalised by the increased oxidation rate, and subsequent fragmentation, of aminoferrocene 6 at these high temperatures *via* known oxidation pathways.³⁷ To minimise product oxidation, all subsequent assays were performed at room temperature. Importantly however, at all temperatures tested, minimal background conversions were observed (<2%),

which reinforces the high stability of the carbamate functionality to undesired background hydrolysis.

The optimised assay parameters were then applied to the detection of different H_2O_2 concentrations using probe 1 (Fig. 8) and a calibration curve obtained (Fig. 9). Overall, the optimisation allowed for near quantitative conversions to aminoferrocene 6 to be achieved in just 20 minutes in the presence of 10 equivalents of H_2O_2 and importantly, in the absence of any peroxide, no conversion was seen. A linear dynamic range between 0 and 800 μM of H_2O_2 could also be observed.

Peroxide selectivity studies

To determine the selectivity of the probe for H_2O_2 , a range of different peroxides, oxidants and salts were screened (Fig. 10). Specifically, a 100 μM solution of probe 1 was exposed to 5 equivalents of the oxidant and after 20 minutes of vigorous stirring, a sample of the assay was taken and subjected to DPV analysis. Of all oxidants screened, sodium percarbonate was the only oxidant other than H_2O_2 to give >15% conversion of

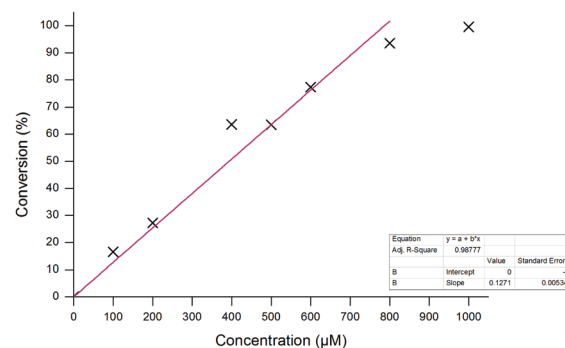


Fig. 9 Calibration curve for the conversion of probe 1 (100 μM) to aminoferrocene 6 after 20 minutes at varying H_2O_2 concentrations.



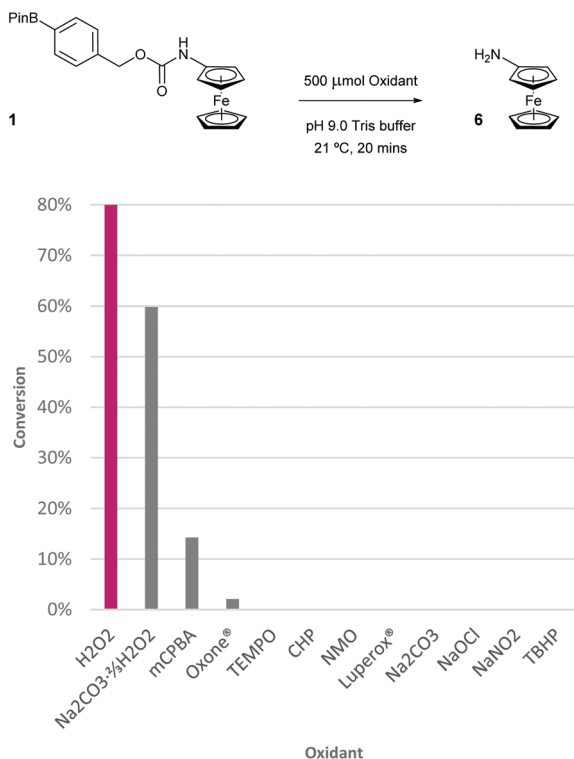


Fig. 10 Conversion of probe **1** (100 μM) to aminoferrocene **6** in 50 mM pH 9.0 Tris buffer in the presence of 500 μM of varying oxidants at room temperature. Abbreviations: *m*CPBA = *meta*-chloroperbenzoic acid, Oxone® = potassium peroxymonosulfate, TEMPO = 2,2,6,6-tetramethyl-1-piperidinyloxy, CHP = cumene hydroperoxide, NMO = 4-methylmorpholine *N*-oxide, Luperox® = di-*tert*-butyl peroxide, TBHP = *tert*-butylhydrogen peroxide.

probe **1** to aminoferrocene **6**. Sodium carbonate itself delivered 0% confirming that the conversion observed for sodium percarbonate is caused by the ≈66% contained H₂O₂. *meta*-Chloroperbenzoic acid (*m*CPBA) furnished 14% conversion over the same time period but significant decomposition of both **1** and **6** was observed in this case, presumably due to oxidation of the iron(II) centre. Other peroxides, such as Oxone®, cumene hydroperoxide (CHP), Luperox® and *tert*-butylhydrogen peroxide (TBHP), all gave little to no conversion showing the excellent selectivity of probe **1** to H₂O₂. Other ROS, including free radicals (TEMPO), *N*-oxides (NMO), hypochlorite and nitrite, among others (see ESI† for full oxidant screen), also afforded minimal conversion if any.

Ratiometric electrochemical glucose detection

According to the World Health Organisation, an estimated 422 million people suffer with diabetes globally and approximately 90% suffer with Type II; the type most commonly caused by behavioural and environmental risk factors.³⁸ Left unregulated, elevated blood glucose levels can inflict significant capillary vessel damage and, depending on its location in the body, can go on to cause retinopathy, kidney failure and the onset of cardiovascular disease.³⁹ Evidently, glucose con-

centrations in blood needs to be regularly measured reliably and to a high level of accuracy ($\pm 20\%$ for concentrations above 5.6 mM or within ± 0.83 mM for below).⁴⁰ Surprisingly however, many currently commercially available glucose biosensors do not meet this standard.⁴¹ There is therefore still significant room for improvement regarding improving the accuracy and reliability of glucose detection.

Selective enzymatic reactions are often employed within electrochemical analyte detection methods to minimise noise from the possible presence of electrooxidisable interferents in the sample matrix.⁴² For electrochemical glucose sensing, glucose oxidase (GOx) is most commonly chosen,⁴³ and in the process of oxidising glucose to *D*-glucono- δ -lactone, the mechanism of action for GOx also reduces molecular oxygen to hydrogen peroxide (H₂O₂).⁴⁴ As such, we hypothesised that we could also apply probe **1** under our previously optimised conditions towards the ratiometric electrochemical detection of glucose.

Initially, we sought to investigate the level of GOx activity needed to achieve full conversion of probe **1** in the shortest time (see ESI†), to help facilitate implementation of the methodology into a point-of-need device in the future. The concentration of glucose within the assay was chosen to be 5 mM (50 eq.) to ensure that enough H₂O₂ would be released to deliver full conversion of **1**. As expected, high levels of GOx activity (>50 U mL⁻¹) delivered full conversion of **1** to **6** within the 20-minute assay time. Lowering the concentration of the enzyme led to a much slower conversion since the rate of glucose oxidation, and therefore H₂O₂ production, would be greatly reduced. Importantly, in the absence of GOx, neither conversion of **1** to aminoferrocene **6**, or any shift in oxidation potential,⁴⁵ was observed showing that conversion of the probe was not occurring through a supramolecular interaction between the boronic acid ester and glucose.⁴⁶

As both high sensitivity for the analyte and a quick time-to-response are both critical factors in the implementation of diagnostic assays within point-of-need biosensors, we chose to take forward the highest concentration of GOx previously tested. Thus, to attain the sensitivity of the ratiometric electrochemical assay towards glucose, a range of glucose concentrations were screened in the presence of 100 U mL⁻¹ GOx (Fig. 11).

Similar to previous, high concentrations of glucose (>5 mM) were able to successfully achieve full conversion of probe **1** to **6** within the 20-minute timeframe. Again, in the absence of the sugar, no conversion was observed which highlights the selectivity of the probe towards the enzyme-catalysed production of H₂O₂ and not through any undesired interaction with the enzyme. The assay also demonstrated a good dynamic range over two orders of magnitude allowing for glucose concentrations between 10 μM and 1 mM to be easily distinguishable after just 10 minutes (Fig. 12). Glucose concentrations in blood, and other bodily fluids, are typically found within this range,⁴⁷ which lends this ratiometric detection method towards such application if desired. As all ratiometric electrochemical conversions have been determined through the use



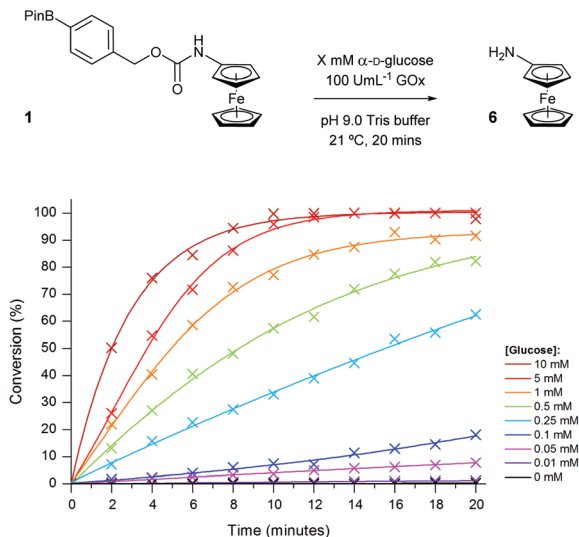


Fig. 11 Conversion of probe 1 (100 μ M) to aminoferrocene 6 in 50 mM pH 9.0 Tris buffer in the presence of 100 U mL⁻¹ GOx with varying concentrations of α -D-glucose.

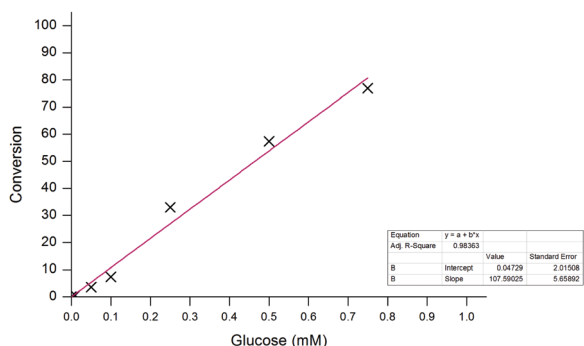


Fig. 12 Calibration curve for the conversion of probe 1 (100 μ M) to aminoferrocene 6 after 10 minutes.

of screen-printed carbon electrodes, subsequent work will involve the implementation of the methodology into a point-of-need biosensor with the aim of developing a device with an improved accuracy over those which are currently commercially available.

Conclusions

In conclusion, two ferrocene-derived probes were designed for the ratiometric electrochemical detection of hydrogen peroxide (H_2O_2) and synthesised to contain two different self-immolative linkers for comparison. The probe containing a benzyl carbamate linker was found to give a larger difference in oxidation potential between probe and product and exhibited faster elimination kinetics than the probe containing an allyl carbamate linker. An optimisation of the diagnostic assay parameters found that pH 9 tris(hydroxymethyl)methylamine (Tris) buffer at room temperature afforded efficient conversion of

probe to product while minimising electrochemical artefacts and any undesired product oxidation. The probe was also found to be very selective for H_2O_2 compared with a range of other common oxidants.

The ratiometric electrochemical detection methodology was then applied to the detection of glucose through the concomitant glucose oxidase (GOx)-catalysed reduction of O_2 to H_2O_2 . The optimum enzyme concentration was initially found prior to the determination of the sensitivity of the glucose assay. Glucose concentrations as low as 50 μ M could be determined from the background rate within 20 minutes and the assay also exhibited a good dynamic range over 2 orders of magnitude.

Acknowledgements

The authors would like to thank Atlas Genetics Ltd for the kind donation of a potentiostat and for providing the screen-printed carbon electrodes. They would also like to acknowledge the use of nuclear magnetic resonance (NMR) and mass spectrometry (MS) facilities within the Chemical Characterisation and Analysis Facility (CCAF) at the University of Bath for compound characterisation.

Notes and references

- C. W. Jones, *Applications of Hydrogen Peroxide and Derivatives*, The Royal Society of Chemistry, Cambridge, 1999, ch. 6, pp. 231–251.
- (a) Z. A. Wood, L. B. Poole and P. A. Karplus, *Science*, 2003, **300**, 650; (b) S. G. Rhee, *Science*, 2006, **312**, 1882; (c) E. A. Veal, A. M. Day and B. A. Morgan, *Mol. Cell*, 2007, **26**, 1.
- (a) S. K. Jonas, P. A. Riley and R. L. Willson, *Biochem. J.*, 1989, **264**, 651; (b) A. M. Gardner, F.-H. Xu, C. Fady, F. J. Jacoby, D. C. Duffey, Y. Tu and A. Lichtenstein, *Free Radical Biol. Med.*, 1997, **22**, 73; (c) C. Richter-Landsberg and U. Vollgraf, *Exp. Cell Res.*, 1998, **244**, 218; (d) U. Vollgraf, M. Wegner and C. Richter-Landsberg, *J. Neurochem.*, 1999, **73**, 2501; (e) P. Daroui, S. D. Desai, T.-K. Li, A. A. Liu and L. F. Liu, *J. Biol. Chem.*, 2004, **279**, 14587.
- (a) R. G. Zepp, B. C. Faust and J. Hoigne, *Environ. Sci. Technol.*, 1992, **26**, 313; (b) Y. Sun and J. J. Pignatello, *Environ. Sci. Technol.*, 1993, **27**, 304; (c) M. I. Stefan, A. R. Hoy and J. R. Bolton, *Environ. Sci. Technol.*, 1996, **30**, 2382.
- C. C. Winterbourn, *Nat. Chem. Biol.*, 2008, **4**, 278.
- (a) T. Finkel and N. J. Holbrook, *Nature*, 2000, **408**, 239; (b) M. Giorgio, M. Trinei, E. Miglaccio and P. G. Pelicci, *Nat. Rev. Mol. Cell Biol.*, 2007, **8**, 722; (c) M. T. Lin and M. F. Beal, *Nature*, 2006, **443**, 787; (d) N. Houstis, E. D. Rosen and E. S. Lander, *Nature*, 2006, **440**, 944;



- (e) J. P. Fruehauf and F. L. Meysken Jr., *Clin. Cancer Res.*, 2007, **448**, 789.
- 7 A. M. Azevedo, D. M. F. Prazeres, J. M. S. Cabral and L. P. Fonseca, *Biosens. Bioelectron.*, 2005, **21**, 235.
- 8 K. Kahn, P. Serfozo and P. A. Tipton, *J. Am. Chem. Soc.*, 1997, **119**, 5435.
- 9 M. S. Pilone, *Cell. Mol. Life Sci.*, 2000, **57**, 1732.
- 10 E. W. van Hellemond, N. G. H. Leferink, D. P. H. M. Heuts, M. W. Fraaije and W. J. H. van Berkel, *Advances in Applied Microbiology*, Elsevier, San Diego, 2006, vol. 60, ch. 2, pp. 17–45.
- 11 R. Wilson and A. P. F. Turner, *Biosens. Bioelectron.*, 1992, **7**, 165.
- 12 For reviews: (a) P. Scrimin and L. J. Prins, *Chem. Soc. Rev.*, 2011, **40**, 4488; (b) O. V. Makhlynets and I. V. Korendovych, *Biomolecules*, 2014, **4**, 402; (c) S. Goggins and C. G. Frost, *Analyst*, 2016, **141**, 3157.
- 13 For specific examples: (a) E. Sella and D. Shabat, *J. Am. Chem. Soc.*, 2009, **131**, 9934; (b) M. Avital-Shmilovici and D. Shabat, *Bioorg. Med. Chem.*, 2010, **18**, 3643; (c) E. Sella, A. Lubelski, J. Klafter and D. Shabat, *J. Am. Chem. Soc.*, 2010, **132**, 3945; (d) N. Karton-Lifshin and D. Shabat, *New J. Chem.*, 2012, **36**, 386; (e) K. Yeung, K. M. Schmid and S. T. Phillips, *Chem. Commun.*, 2013, **49**, 394; (f) E. Sella and D. Shabat, *Org. Biomol. Chem.*, 2013, **11**, 5074; (g) T. Yoshii, S. Onogi, H. Shigemitsu and I. Hamachi, *J. Am. Chem. Soc.*, 2015, **137**, 3360.
- 14 Y. Salinas, R. Martínez-Máñez, M. D. Marcos, F. Sancenón, A. M. Costero, M. Parra and S. Gil, *Chem. Soc. Rev.*, 2012, **41**, 1261.
- 15 (a) M. Schäferling, D. B. M. Grögel and S. Schreml, *Microchim. Acta*, 2011, **174**, 1; (b) O. S. Wolfbeis, A. Dürkop, M. Wu and Z. Lin, *Angew. Chem., Int. Ed.*, 2002, **41**, 4495; (c) Y.-C. Shiang, C.-C. Huang and H.-T. Chang, *Chem. Commun.*, 2009, 3437; (d) O. Seven, F. Sozmen and I. S. Turan, *Sens. Actuators, B*, 2017, **239**, 1318.
- 16 (a) L.-C. Lo and C.-Y. Chen, *Chem. Commun.*, 2003, 2728; (b) A. E. Albers, V. S. Okreglak and C. J. Chang, *J. Am. Chem. Soc.*, 2006, **128**, 9640; (c) B. C. Dickinson, C. Huynh and C. J. Chang, *J. Am. Chem. Soc.*, 2010, **132**, 5906; (d) N. Karton-Lifshin, E. Segal, L. Omer, M. Portnoy, R. Satchi-Fainaro and D. Shabat, *J. Am. Chem. Soc.*, 2011, **133**, 10960; (e) D. Srikun, E. W. Miller, D. W. Domaille and C. J. Chang, *J. Am. Chem. Soc.*, 2008, **130**, 4596; (f) X. Sun, S.-Y. Xu, S. E. Flower, J. S. Fossey, X. Qian and T. D. James, *Chem. Commun.*, 2013, **49**, 8311; (g) X. Sun, M. Odyniec, A. C. Sedgwick, K. Lacina, S. Xu, T. Qiang, S. Bull, F. Marken and T. D. James, *Org. Chem. Front.*, 2017, DOI: 10.1039/C6QO00448B.
- 17 (a) J. Wang, *Biosens. Bioelectron.*, 2006, **21**, 1887; (b) N. J. Ronkainen, H. B. Halsall and W. R. Heineman, *Chem. Soc. Rev.*, 2010, **39**, 1747.
- 18 (a) Y. Du, B. J. Lim, B. Li, Y. S. Jiang, J. L. Sessler and A. D. Ellington, *Anal. Chem.*, 2014, **86**, 8010; (b) F. Gao, L. Du, Y. Zhang, D. Tang and Y. Du, *Anal. Chim. Acta*, 2015, **883**, 67; (c) E. Xiong, X. Zhang, Y. Liu, J. Zhou, P. Yu, X. Li and J. Chen, *Anal. Chem.*, 2015, **87**, 7291; (d) T. Wang, L. Zhou, S. Bai, Z. Zhang, J. Li, X. Jing and G. Xie, *Biosens. Bioelectron.*, 2016, **78**, 464; (e) B. Wei, J. Zhang, H. Wang and F. Xia, *Analyst*, 2016, **141**, 4313.
- 19 (a) A. Sagi, J. Rishpon and D. Shabat, *Anal. Chem.*, 2006, **78**, 1459; (b) S. Goggins, B. J. Marsh, A. T. Lubben and C. G. Frost, *Chem. Sci.*, 2015, **6**, 4978; (c) X. Cao, J. Xia, H. Liu, F. Zhang, Z. Wang and L. Lu, *Sens. Actuators, B*, 2017, **239**, 166.
- 20 (a) K. Ren, J. Wu, F. Yan and H. Ju, *Sci. Rep.*, 2014, **4**, 4360; (b) P. Yu, J. Zhou, L. Wu, E. Xiong, X. Zhang and J. Chen, *J. Electroanal. Chem.*, 2014, **732**, 61; (c) K. Ren, J. Wu, F. Yan, Y. Zhang and H. Ju, *Biosens. Bioelectron.*, 2015, **66**, 345; (d) P. Yu, X. Zhang, J. Zhou, E. Xiong, X. Li and J. Chen, *Sci. Rep.*, 2015, **5**, 16015; (e) F. Gao, Y. Qian, L. Zhang, S. Dai, Y. Lan, Y. Zhang, L. Du and D. Tang, *Biosens. Bioelectron.*, 2015, **71**, 158; (f) S. Goggins, C. Naz, B. J. Marsh and C. G. Frost, *Chem. Commun.*, 2015, **51**, 561; (g) Y. Liu, Y. Liu, Z. Matharu, A. Rahimian and A. Revzin, *Biosens. Bioelectron.*, 2015, **64**, 43; (h) C. Deng, X. Pi, P. Qian, X. Chen, W. Wu and J. Xiang, *Anal. Chem.*, 2017, **89**, 966.
- 21 (a) X. Chai, L. Zhang and Y. Tian, *Anal. Chem.*, 2014, **86**, 10668; (b) E. Xiong, L. Wu, J. Zhou, P. Yu, X. Zhang and J. Chen, *Anal. Chim. Acta*, 2015, **853**, 242; (c) J. Jia, H. G. Chen, J. Feng, J. L. Lei, H. Q. Luo and N. B. Li, *Anal. Chim. Acta*, 2016, **908**, 95.
- 22 (a) H. Cheng, X. Wang and H. Wei, *Anal. Chem.*, 2015, **87**, 8889; (b) X. Zhang, L. Wu, J. Zhou, X. Zhang and J. Chen, *J. Electroanal. Chem.*, 2015, **742**, 97; (c) P. Yeng, Y. Liu, X. Zhang, J. Zhou, E. Xiong, X. Li and J. Chen, *Biosens. Bioelectron.*, 2016, **79**, 22; (d) Y. Liu, X. Zhang, J. Yang, E. Xiong, X. Zhang and J. Chen, *Can. J. Chem.*, 2016, **94**, 509; (e) M. Kesavan, V. Mani and S.-T. Huang, *RSC Adv.*, 2016, **6**, 71727; (f) H. Li, N. Arroyo-Currás, D. King, F. Ricci and K. W. Plaxco, *J. Am. Chem. Soc.*, 2016, **138**, 15809.
- 23 W.-J. Shen, Y. Zhuo, Y.-Q. Chai and R. Yuan, *Anal. Chem.*, 2015, **87**, 11345.
- 24 S. Alegret, F. Céspedes, E. Martínez-Fàbregas, D. Martorell, A. Morales, E. Centelles and J. Muñoz, *Biosens. Bioelectron.*, 1996, **11**, 35.
- 25 W. Chen, S. Cai, Q.-Q. Ren, W. Wen and Y.-D. Zhao, *Analyst*, 2012, **137**, 49.
- 26 A. R. Lippert, G. C. van de Bittner and C. J. Chang, *Acc. Chem. Res.*, 2011, **44**, 793.
- 27 D.-G. Cho and J. L. Sessler, *Chem. Soc. Rev.*, 2009, **38**, 1647.
- 28 J. L. Major Jourden, K. B. Daniel and S. M. Cohen, *Chem. Commun.*, 2011, **47**, 7968.
- 29 S. Gnaim and D. Shabat, *Acc. Chem. Res.*, 2014, **47**, 2970.
- 30 A. D. Brooks, K. Yeung, G. G. Lewis and S. T. Phillips, *Anal. Methods*, 2015, **7**, 7186.
- 31 D. C. D. Butler and C. J. Richards, *Organometallics*, 2002, **21**, 5433.
- 32 (a) A. N. Nesmeyanov, V. A. Sazonova and V. N. Drozd, *Tetrahedron Lett.*, 1959, **1**, 13; (b) R. Epton, G. Marr and G. K. Rogers, *J. Organomet. Chem.*, 1976, **110**, C42.



- 33 C. J. McNeil, I. J. Higgins and J. V. Bannister, *Biosensors*, 1987/88, **3**, 199.
- 34 B. J. Marsh, L. Hampton, S. Goggins and C. G. Frost, *New J. Chem.*, 2014, **38**, 5260.
- 35 A. Alouane, R. Labruère, T. Le Saux, F. Schmidt and L. Jullien, *Angew. Chem., Int. Ed.*, 2015, **54**, 7492.
- 36 R. G. Bates and V. E. Bower, *Anal. Chem.*, 1956, **28**, 1322.
- 37 (a) H. Hagan, P. Marzenell, E. Jentzsch, F. Wenz, M. R. Veldwijk and A. Mokhir, *J. Med. Chem.*, 2012, **55**, 924; (b) P. Marzenell, H. Hagan, L. Sellner, T. Zenz, R. Grinyte, V. Pavlov, S. Daum and A. Mokhir, *J. Med. Chem.*, 2013, **56**, 6935; (c) A. Leonidova, P. Anstaett, V. Pierroz, C. Mari, B. Spingler, S. Ferrari and G. Gasser, *Inorg. Chem.*, 2015, **54**, 9740; (d) M. Schikora, A. Reznikov, L. Chaykovskaya, O. Sachinska, L. Polyakova and A. Mokhir, *Bioorg. Med. Chem. Lett.*, 2015, **25**, 3447.
- 38 *Global Report on Diabetes*, World Health Organisation (WHO), Geneva, 2016.
- 39 D. M. Nathan, *N. Engl. J. Med.*, 1993, **328**, 1676.
- 40 *In Vitro Diagnostic Test Systems – Requirements for Blood Glucose Monitoring Systems for Self-Testing in Managing Diabetes Mellitus (ISO 15197:2013)*, International Organisation for Standardisation (ISO), Geneva, 2013.
- 41 C. Tack, H. Pohlmeier, T. Behnke, V. Schmid, M. Grenningloh, T. Forst and A. Pfützner, *Diabetes Technol. Ther.*, 2012, **14**, 330.
- 42 A. Heller and B. Feldman, *Chem. Rev.*, 2008, **108**, 2482.
- 43 R. Wilson and A. P. F. Turner, *Biosens. Bioelectron.*, 1992, **7**, 165.
- 44 S. B. Bankar, M. V. Bule, R. S. Singhal and L. Ananthanarayan, *Biotechnol. Adv.*, 2009, **27**, 489.
- 45 H.-C. Wang, H. Zhou, B. Chen, P. M. Mendes, J. S. Fossey, T. D. James and Y.-T. Long, *Analyst*, 2013, **138**, 7146.
- 46 X. Sun and T. D. James, *Chem. Rev.*, 2015, **115**, 8001.
- 47 E. Witkowska Nery, M. Kundys, P. S. Jeleń and M. Jönsson-Niedziółka, *Anal. Chem.*, 2016, **88**, 11271.

